UC San Diego
UC San Diego Previously Published Works

Title

Hippo-independent activation of YAP by the GNAQ uveal melanoma oncogene through a trio-regulated rho GTPase signaling circuitry.

Permalink

https://escholarship.org/uc/item/29g2c00t

Journal

Cancer Cell, 25(6)

Authors

Feng, Xiaodong
Degese, Maria
Iglesias-Bartolome, Ramiro
et al.

Publication Date

2014-06-16

DOI

10.1016/j.ccr.2014.04.016

Peer reviewed

Hippo-Independent Activation of YAP by the *GNAQ* Uveal Melanoma Oncogene through a Trio-regulated Rho GTPase Signaling Circuitry

Xiaodong Feng[1,2], **Maria Sol Degese**[1], **Ramiro Iglesias-Bartolome**[1], **Jose P. Vaque**[1], **Alfredo A. Molinolo**[1], **Murilo Rodrigues**[3], **M. Raza Zaidi**[4], **Bruce R. Ksander**[5], **Glenn Merlino**[6], **Akrit Sodhi**[3], **Qianming Chen**[2,*], and **J. Silvio Gutkind**[1,*]

[1]Oral and Pharyngeal Cancer Branch, National Institute of Dental and Craniofacial Research, National Institutes of Health, Bethesda, MD 20892-4340, USA

[2]State Key Laboratory of Oral Diseases, West China Hospital of Stomatology, Sichuan University, Chengdu, Sichuan 610041, China

[3]Wilmer Eye Institute, Johns Hopkins School of Medicine, Baltimore, MD 21287

[4]Fels Institute for Cancer Research and Molecular Biology, Temple University School of Medicine, Philadelphia, PA 19140, USA

[5]Schepens Eye Research Institute, Harvard Medical School, Boston, MA 02114, USA

[6]Laboratory of Cancer Biology and Genetics, National Cancer Institute, Bethesda, Maryland 20892, USA

Summary

Mutually exclusive activating mutations in the *GNAQ* and *GNA11* oncogenes, encoding heterotrimeric Gαq family members, have been identified in ~83% and ~6% of uveal and skin melanomas, respectively. However, the molecular events underlying these *GNAQ*-driven malignancies are not yet defined, thus limiting the ability to develop cancer-targeted therapies. Here, we focused on the transcriptional co-activator YAP, a critical component of the Hippo signaling pathway that controls organ size. We found that Gαq stimulates YAP through a Trio-Rho/Rac signaling circuitry promoting actin polymerization, independently of PLCβ and the canonical Hippo pathway. Furthermore, we show that Gαq promotes the YAP-dependent growth of uveal melanoma cells, thereby identifying YAP as a suitable therapeutic target in uveal melanoma, the first described *GNAQ*/*GNA11*-initiated human malignancy.

*QC, Correspondence: qmchen@scu.edu.cn. *JSG, Correspondence: sg39v@nih.gov.

Keywords

GNAQ; *GNA11*; G proteins; YAP; Rho; Rac; Hippo pathway; melanoma

Introduction

Mutations in *GNAQ* and *GNA11*, encoding two members of the Gαq family of heterotrimeric G protein α subunits, Gαq and Gα11, respectively, occur in roughly 5% of all tumors sequenced to date (O'Hayre et al., 2013). The majority of these mutations affect residues Q209 and R183, which are required for Gα$_q$ GTPase activity (Berman et al., 1996; Van Raamsdonk et al., 2010). Thus, the most frequent mutations observed in *GNAQ* and *GNA11* render them GTPase defective and constitutively active, leading to prolonged signaling. Of interest, ~83% of ocular melanomas harbor mutations in *GNAQ* or *GNA11*, where they are now considered to represent the driver oncogenes (Van Raamsdonk et al., 2009; Van Raamsdonk et al., 2010). This provides a clear example of a human malignancy that is initiated by gain of function mutations in Gα$_q$ and Gα$_{11}$ proteins. Although less studied, *GNAQ* and *GNA11* mutations are also frequently found in leptomeningeal melanocytomas (50%) and melanomas (25%) arising from the meninges (Kusters-Vandevelde et al., 2010), in most blue nevi of the skin (83%), and in a subset (6%) of cutaneous melanomas (Van Raamsdonk et al., 2009).

The best-known downstream signaling event initiated by Gαq involves its ability is to activate phospholipase C (PLC) β and the consequent increased hydrolysis of phosphatidylinositol 4,5-bisphosphate (PIP$_2$) to produce two second messengers: inositol 1,4,5-trisphosphate (IP$_3$) and diacylglycerol (DAG) (Hubbard and Hepler, 2006). IP$_3$ raises cytoplasmic Ca^{2+} levels, which stimulates multiple calcium-regulated pathways and, together with DAG, activates classic protein kinase C (PKC) isoforms (Griner and Kazanietz, 2007). However, the molecular events underlying *GNAQ*-driven malignancies are not yet defined, thus limiting the ability to develop novel anticancer-targeted therapies. Here, we focused on the transcriptional co-activator YAP, a critical component of the Hippo signaling pathway, which controls organ size in mammals (Pan, 2010; Ramos and Camargo, 2012; Sudol et al., 1995; Zhao et al., 2010). YAP is active in most proliferating cells, but upon reaching the appropriate cell density, signaling pathways initiated upon cell-cell contact and/or from the organ size-sensing machinery lead to the activation of the Hippo kinase cascade, resulting in the inhibitory activity of the mammalian STE20-like protein kinase 1 (MST1) and MST2, which are the mammalian homologues of Hippo in *Drosophila melanogaster* (Pan, 2010; Ramos and Camargo, 2012; Zhao et al., 2010). This pathway converges in the activation of a kinase known as large tumor suppressor homologue 1 and 2 (LATS1 and LATS2 in humans), which phosphorylates YAP in serine 127, thereby targeting it for retention and degradation in the cytosol, thus limiting its transcriptional activity and resulting in growth inhibition (Camargo et al., 2007; Dong et al., 2007; Pan, 2010; Ramos and Camargo, 2012).

In this study, we show that activating mutation of Gαq can trigger YAP translocation into the nucleus and stimulates YAP-dependent transcription, and that this process is

independent from PLCβ stimulation but requires the activation of a Gαq-regulated guanine nucleotide exchange factor, Trio, and the subsequent activation of the small GTPases RhoA and Rac1 and their associated signaling networks. In turn, this Gαq-Trio-Rho/Rac signaling circuitry contributes to the YAP-dependent growth in uveal melanoma, thus identifying suitable therapeutic targets for uveal melanoma treatment.

Results

YAP activation downstream of oncogenic activating mutants of Gαq (GαqQL) through RhoA and Rac1

To assess the expression and localization of the transcriptional co-activator, YAP, in response to activating mutations in *GNAQ*, we transfected HEK-293 cells with HA-tagged GαqQL (Q209L), one of the most frequent *GNAQ* mutants in uveal melanoma (O'Hayre et al., 2013), using empty vector and wild type Gαq as controls. Both tagged G protein α subunits were expressed at similar levels (Figure 1A) but only the active Gαq protein promoted the nuclear translocation of YAP, as judged by its increased recovery in the nuclear fraction (Figure 1B) and by YAP immune detection in the nucleus of transfected cells, which could be recognized by staining of the HA tag in the background of unstransfected cells (Figure 1C and D). GαqQL also caused a remarkable increase in the luciferase activity of a YAP reporter system driven by a TEAD4-Gal4 chimera, which included the TEAD4 transactivation and YAP-binding domain, and promoted the expression of endogenous YAP-regulated genes, including *CTGF* and *CYR61* (Figure 1E, and Figure S1A). These results, together with recently reported biochemical studies (Yu et al., 2012), support that *GNAQ* activating signaling can lead to YAP nuclear translocation and YAP-dependent activating gene transcription.

However, it is unclear which of the multiple Gαq-initiated pathways regulate YAP, and how the interplay between YAP and other *GNAQ*-initiated signaling pathways contribute to the transduction of proliferative cues by this G protein and its coupled receptors. The activation of PLCβ is one of the best-known downstream events stimulated by Gαq. Inhibition of PLCβ by the use of a small molecule PLC inhibitor (PLCi) abolished the generation of diffusible second messengers but did not affect the transcriptional activation of YAP by Gαq (Figure 1F and Figure S1B), demonstrating that activation of YAP may be independent of PLCβ.

In a recent study, a genome wide dsRNA screen in drosophila cells revealed that Trio, a highly conserved guanine nucleotide exchange factor, is essential for transducing signals from Gαq to the AP1 transcription factors through the activation of Rho-GTPases and their signaling circuitries (Vaque et al., 2013). These findings prompted us to investigate whether Trio and its regulated Rho GTPases, RhoA and Rac1, participate in the nuclear translocation and activation of YAP in response to Gαq activating mutations. Knock down of Trio did not affect the expression levels of GαqQL, but abolished its ability to promote the accumulation of activated RhoA and Rac1 (Figure 1G). Knock down of Trio also prevented the activation of the YAP transcriptional activity caused by GαqQL (Figure 1H and Figure S1C). However, while the activation of YAP by activated RhoA has been recently reported (Yu et al., 2012), we observed that Rac1 can also stimulate the nuclear translocation of endogenous

YAP and its transactivating activity when expressed together with the GAL4-TEAD4 reporter system (Figure 1I–M). Interestingly, knockdown of either of these two Rho-GTPases prevented the transcriptional activation of YAP induced by GαqQL (Figure 1N and Figure S1D–E). Thus, while the activated mutants of either RhoA or Rac1 can activate YAP, the concomitant activation of both endogenous GTPases appears to be required for the full stimulation of endogenous YAP when activated by oncogenic forms of Gαq.

Conditional expression of the *GNAQ* oncogene promotes melanoma formation and YAP activation *in vivo*

To investigate whether activated *GNAQ* can drive melanocyte transformation *in vivo*, we generated a mouse model expressing HA-GαqQL under the control of the *tet*-responsive elements (tet-HA-GαqQL) and bred them with mice expressing the reverse tetracycline-activated transactivator rtTA2, regulated by the melanocyte-specific dopachrome tautomerase (*Dct*) gene promoter (*Dct-rtTA*) (Zaidi et al., 2011). Initially, we used the nuclear expression of a *tet*-driven H2B-GFP to document the targeted expression to skin melanocytes by *Dct-rtTA* (Figure 2A and B), as previously reported (Zaidi et al., 2011). The *tet-HA-GαqQL* and *Dct-rtTA* transgenic mice were also bred with mice defective in p16^{Ink4a} and p19^{Ink4b} (*p16p19*KO) (Figure 2C), as genetic and epigenetic inactivation of this tumor suppressive pathway is a frequent event in uveal and cutaneous melanoma (Castellano et al., 1997; van der Velden et al., 2001). This was reflected by the methylation of the *Ink4 (CDKN2)* gene promoter region in a representative panel of human melanoma cells lines (Figure S2). Using this animal model system, we observed that when HA-GαqQL was expressed in response to doxycycline treatment in the *p16p19*KO background, more than 50% of the mice develop cutaneous lesions of melanocytic origin expressing Dct (Figure 2D and E and data not shown). This is aligned with the finding that hot spot mutations in *GNAQ* and its related *GNA11* are mutated in 5% of all cutaneous melanomas (O'Hayre et al., 2013; Van Raamsdonk et al., 2009), which based on our observations may represent a tumor-initiating genetic event. In these lesions, most HA-GαqQL expressing cells exhibit nuclear YAP, in contrast to normal tissues in which control GFP expressing melanocytes exhibit cytoplasmic YAP (Figure 2F and G). Thus, mutated *GNAQ* can initiate melanocyte transformation and tumor formation in mice when expressed in a progenitor cell compartment, and results in YAP nuclear localization *in vivo*. As *GNAQ* mutations have been identified in other tumors, we expressed HAGαqQL in the skin, including the hair follicle stem cells, using a cytokeratin 5 (*K5*) *rtTA* diver (Figure 2H) (Vitale-Cross et al., 2004). These mice developed rapid hair loss within days, and exhibited nuclear localization of YAP in epithelial-derived hyperplastic cells in multiple tumor lesions (Figure 2I and J). Collectively, these results suggest that YAP activation in tumors initiated by activating mutations of Gαq is likely a general event, not restricted to melanocyte progenitor cells and their derived tumors.

Trio and a network of Rho-GTPases mediate YAP activation in uveal melanoma cells harboring *GNAQ* mutations

We next examined the expression of YAP in human uveal melanoma lesions. Consistent with our experimental findings, we observed that YAP accumulates in the nucleus in human uveal melanoma lesions (Figure 3A and B). In contrast, normal melanocytes do not express

nuclear YAP in normal tissues. This suggests that YAP may contribute to the oncogenic pathway initiated by *GNAQ* and *GNA11* activating mutations in human uveal melanomas. Based on these observations, we next asked whether YAP is activated in uveal melanoma cells expressing the *GNAQ* oncogene. Indeed, uveal melanoma cells exhibited clear nuclear localized YAP, which was insensitive to PLC inhibition, similar to HEK293 expressing active Gαq, even when PLCi was used to effectively block phosphatidylinositol hydrolysis (Figure 3C and D). The nuclear localization of YAP was abolished after *GNAQ* knock down in uveal melanoma cell lines (Figure 3E and F). Similarly, knock down of Trio, RhoA and Rac1 prevented the nuclear accumulation of YAP in these cells, and diminished the expression of endogenous YAP-regulated genes, *CTGF* and *CYR61* (Figure 3E–G). These findings support that in uveal melanoma cells harboring *GNAQ* mutations, Gαq primarily signals through Trio to RhoA and Rac1 to promote the nuclear localization and activation of YAP, independent of PLC activation and its downstream regulated events.

Surprisingly, uveal melanoma cells displayed very high levels of total and phosphorylated (serine 127) YAP. The latter likely represents the YAP inactive form upon phosphorylation by LATS1 and LATS2, which are highly expressed in these cells, similar to cutaneous melanoma cells expressing *BRAF* and *NRAS* oncogenes, which served as controls. LATS1 was also recognized by antibodies detecting its phosphorylated form at the hydrophobic motif (T1079) and activation loop (S909) both in uveal melanoma cells and in HEK293 cells expressing *GNAQ* (Figure 4A). *GNAQ* expression in HEK293 cells resulted in the accumulation of dephosphorylated YAP, reflected by the faster migration of YAP in Phos-tag-containing gels, with only dephosphorylated YAP accumulating in the nucleus (Figure 4B). All uveal melanoma cells also accumulated dephosphorylated YAP, albeit they still retained phospho-YAP (Figure 4A and C). Together, these observations suggested that LATS1/LATS2 may remain active in uveal melanoma cells, and raised the possibility that YAP activation by *GNAQ* may involve mechanisms in addition to those described resulting in Hippo pathway inactivation and LATS1/2 inhibition (Yu et al., 2012).

To explore this possibility, we knocked down LATS1/2 in HEK293 cells, which alone induced only a slight increase in YAP transcriptional activity in confluent cells. Interestingly, the *GNAQ* oncogene induced the transcriptional activation of YAP even when the repressing signals converging on LATS1/2 were suppressed by knock down of both human LATS isoforms (Figure 4D–F), supporting that activation of YAP by GαqQL is not solely dependent on the inhibition of the Hippo pathway. Recently, a likely Hippo-independent pathway resulting in the activation of YAP initiated by actin polymerization was described in the context of cell mechanical sensing (Aragona et al., 2013; Dupont et al., 2011; Halder et al., 2012). Aligned with the strong activation of RhoA and Rac by GαqQL, uveal melanoma cells exhibit high levels of phosphorylated cofilin (p-cofilin) (Figure 4G), a downstream target of both of these GTPases (Figure 4H and I). p-Cofilin accumulation results in increased actin polymerization, and the consequent increase in polymerized F-actin and decrease in monomeric G-actin (Bernard, 2007; Pollard and Cooper, 2009). Remarkable, YAP nuclear localization and activity was repressed when blocking actin polymerization by inhibiting ROCK, thereby limiting cofilin phosphorylation specifically downstream from RhoA, or by the direct inhibition of G-actin assembly into F-actin by

latrunculin-A (Figure 4J–M, and Figure S3). Together, these findings suggest that *GNAQ* may stimulate YAP by promoting actin polymerization, rather than by solely inhibiting the canonical Hippo pathway.

A Hippo-independent pathway regulated by actin polymerization contributes to YAP activation in uveal melanoma

We next explored the interplay between the Hippo pathway and actin polymerization in YAP activation. Knock down of LATS1/2 resulted in a remarkable increase in the expression of YAP regulated genes in uveal melanoma cells, further supporting that the Hippo pathway still remains active in these cells, restraining maximal YAP activation (Figure 5A and B). Even when LATS1/2 was knocked down, inhibition of actin polymerization decreased YAP activity, both in uveal melanoma and GαqQL transfected cells (Figure 5B–D), suggesting that F-actin accumulation and LATS inhibition may act in a coordinated fashion. Regarding the former, how actin polymerization results in YAP stimulation is complex and not fully understood (Aragona et al., 2013; Dupont et al., 2011; Halder et al., 2012; Johnson and Halder, 2014). Recent studies suggest that YAP may form many multimeric protein complexes utilizing its WW domains, a Leucine Zipper and PDZ-binding motif (Sudol, 2013; Sudol et al., 2012; Wang et al., 2014). Of interest, these include the association of YAP with a cytoskeletal associated protein, Angiomotin (AMOT), which binds F-actin through an N-terminal region that includes a sequence motif, PPxY, by which AMOT associates with WW domains of YAP (Oka et al., 2012; Chan et al., 2013; Dai et al., 2013). We reasoned that F-actin may prevent AMOT associating with YAP, and that upon inhibition of actin polymerization, YAP may be sequestered in an inactive, AMOT-associated pool. Preventing actin polymerization in uveal melanoma cells did not enhance protein complex formation between flag-tagged YAP and endogenous LATS or 14-3-3, both of which repress YAP function (Figure 5E). Instead, YAP association with the endogenous p130 form of AMOT was increased after inhibition of actin polymerization (Figure 5E). This could be recapitulated *in vitro*, as AMOT bound to flag-YAP was competed out by incubating the immunoprecipitates with F-actin but not G-actin (Figure 5F). Consistently, AMOT knock down had limited impact on YAP-dependent gene expression in uveal melanoma cells, as it is expected to bind YAP poorly in the presence of cytosolic F-actin, but AMOT knock down rescued YAP function inhibition caused by actin depolymerization (Figure 5G and H). Taken together, these findings suggest that in uveal melanoma cells F-actin accumulation causes the dissociation of AMOT-YAP complexes, thereby contributing to YAP nuclear translocation and YAP-dependent transcription (Figure 5I).

YAP represents a therapeutic target in uveal melanoma

We next explored the role of YAP activation in uveal melanoma tumor formation. For these studies, we established lentiviral delivered shRNAs knocking down YAP and control shRNA in uveal melanoma cells. This approach revealed that YAP knock down resulted in reduced YAP-dependent expression of typical YAP-regulated genes (Mo et al., 2012) and decreased proliferation of uveal melanoma cells (Figure 6A–C). Furthermore, knock down of YAP led to reduced number of colonies in uveal melanoma cells cultured in 3D matrix, as well as a reduced colony size (Figure 6D). Taking advantage of the ability to establish uveal melanoma xenografts in immune compromised mice, we observed that YAP knockdown

reduced tumor size *in vivo* (Figure 6E). Taken together, these results suggest that YAP activation may represent a molecular event involved in uveal melanoma tumor growth *in vitro* and *in vivo*.

These observations raised the possibility that YAP may represent a therapeutic target for the treatment of patients with uveal melanoma. Based on the identification of VP (verteporfin) as a potent inhibitor of the YAP/TEAD4 interaction in a recent high throughput drug screen (Liu-Chittenden et al., 2012), we asked whether VP can exert an antitumoral activity in uveal melanoma cell lines. VP treatment reduced colony formation and proliferation of uveal melanoma cells in soft agar 3D cultures (Figure 6F) and dramatically reduces uveal melanoma cell tumorigenesis and proliferation *in vivo* (Figure 6G and H). These results suggest that the pharmacological inhibition of YAP by VP may represent as a therapeutic approach for the treatment of patients with uveal melanomas.

Discussion

Recent large cancer sequencing efforts have revealed an unexpected high frequency of gain of function mutations in heterotrimeric G protein α-subunits (O'Hayre et al., 2013). Among them, mutations in the *GNAQ* oncogenes, *GNAQ* and *GNA11*, are now believed to represent the genetic initiating event in uveal melanomas, and in a subset of melanomas arising in the skin (Van Raamsdonk et al., 2009; Van Raamsdonk et al., 2010) among other tumors. In this study, we show that YAP activation represents a key molecular event contributing to *GNAQ*-induced tumorigenesis, which is dependent on the activation of Trio and its regulated Rho GTPases, RhoA and Rac1, in uveal melanoma cells harboring activating *GNAQ* mutations. Furthermore, we provide evidence that YAP activation may involve, at least in part, a Hippo-independent pathway impinging on the regulation of the actin cytoskeleton by Rho GTPases. These findings suggest that inhibition of YAP function may represent a suitable pharmacological intervention strategy in uveal melanoma and other hyperproliferative lesions that result from gain of function *GNAQ* mutations.

YAP is a transcriptional co-activator that acts as a powerful tumor promoter, and its activation is a frequent event in numerous cancers, including lung, colorectal, ovarian, liver and prostate cancers (Dong et al., 2007; Johnson and Halder, 2014; Zhao et al., 2007). The Hippo pathway is believed to be the major regulator of YAP nuclear localization, activity and tumorigenic potential (Camargo et al., 2007; Dong et al., 2007; Pan, 2010; Ramos and Camargo, 2012; Zhao et al., 2010). YAP and its *D. melanogaster* counterpart Yorkie (YKI), promote tissue growth and cell viability by regulating the activity of different transcription factors, including TEADs and SMADs. In mammals, YAP overexpression or hyperactivation causes excess proliferation in multiple tissues, including the liver, gastrointestinal tract, skin and heart (Camargo et al., 2007; Dong et al., 2007; Schlegelmilch et al., 2011). Despite this, somatic or germline mutations in Hippo pathway genes are uncommon, prompting the exploration of other mechanism(s) underlying YAP activation in each tumor type (Johnson and Halder, 2014).

Recent studies suggest that GPCR signaling can regulate the Hippo pathway (Yu et al., 2012). Specifically, GPCRs linked to $G\alpha_{12/13}$ inhibit the activity of LATS thereby relieving

YAP from the LATS-dependent inhibitory phosphorylation in serine 127 (Yu et al., 2012), while receptors activating Gαs may promote LATS activation thus causing YAP inhibition by increasing Hippo pathway activation. Whether *GNAQ*-activating mutations and the large family of receptors regulating cell growth through Gαq affect the Hippo pathway, however, is much less understood (Yu et al., 2012). In our study, we found that YAP is a key pro-tumorigenic gene in uveal melanoma cells harboring *GNAQ* activating mutations, which is critical for uveal melanoma growth and tumor formation as judged by knock down experiments and by the use of small molecule inhibitors. Moreover, we also showed that activation of YAP downstream from Gαq occurs through the stimulation of Trio and Trio-dependent-Rho GTPases, RhoA and Rac1. Of interest, Gαq activation did not result in decreased levels of phosphorylated LATS and YAP, and Gαq activated YAP further even when LATS was knocked down in both uveal melanoma and HEK293 cells. Instead, our results suggest that Gαq stimulates YAP by a process involving changes in actin dynamics rather than solely on Hippo kinase cascade regulation, resembling recent findings in the context of mechanosensing transduction signals (Aragona et al., 2013; Dupont et al., 2011; Halder et al., 2012).

In this regard, whereas in *Drosophila* most of the key components of the Hippo pathway have been genetically defined, in mammalian cells YAP may receive negative and positive inputs from multiple signaling systems in addition to those described in flies. For example, a recent kinome wide screen in mammalian cells revealed that the tumor suppressor protein LKB1 inhibits YAP by activating the core Hippo kinases, while members of the JNK pathway diminish YAP function independently of Hippo (Mohseni et al., 2014). The regulation of YAP by the cytoskeleton in *Drosophila* involves the tumor suppressor Merlin/NF2, which can cause the activation of *Drosophila* LATS (*Wts*), and hence activate the Hippo pathway diminishing Yki activity upon the disruption of the cytoskeleton (Yin et al., 2013). While this repressive function is also likely performed by NF2 in mammals, the activation of YAP by mechanosensing mechanisms appears not to require LATS inhibition, as supported by multiple experimental approaches (Aragona et al., 2013; Dupont et al., 2011). Similarly, active Gαq, RhoA, and Rac1 stimulated YAP potently even when endogenous LATS1/2 were efficiently knock down. In line with this possibility, in uveal melanoma cells LATS1 is phosphorylated in its activation loop, while LATS1/2 knockdown results in a remarkable increase in the transcriptional activity of YAP, indicating that these core Hippo kinases retain a restraining activity on YAP function. Instead, disruption of the actin cytoskeleton diminishes both the basal activity of YAP and YAP hyperactivation caused by LATS1/2 reduced expression. Thus, YAP stimulation by *GNAQ* in uveal melanoma cells requires the persistent activation of a cytoskeleton-regulated pathway, which may cooperate with, or bypass the requirement of Hippo pathway inactivation.

The fact that RhoA and Rac1 stimulate YAP, albeit RhoA more potently, may provide some possible hints on the underlying mechanism. While these GTPases often act antagonistically for cell movement, they both converge in the activation of LIMK and the consequent phosphorylation and inactivation of the actin severing protein cofilin, thus favoring actin polymerization and F-actin accumulation (reviewed in (Bar-Sagi and Hall, 2000)). RhoA activates LIMK through ROCK, and Rac1 stimulates this kinase through PAK (reviewed in

(Bar-Sagi and Hall, 2000; Radu et al., 2014), which can explain why ROCK inhibitors do not prevent the activation of YAP by the latter. In turn, how F-actin stimulates YAP was unclear (reviewed in (Matsui and Lai, 2013). YAP is part of multiple cytosolic protein complexes, many of which are driven by the direct interaction between the WW domains of YAP with the PPxY motifs present in most of its associated proteins, including LATS and AMOT (Sudol, 2013; Sudol et al., 2012; Wang et al., 2014). The latter has recently received increased attention, as AMOT represses YAP function (Chan et al., 2011; Zhao et al., 2011) and competes for LATS binding to YAP (Yi et al., 2013), while there are no AMOT orthologs in *Drosophila*, thus representing a fundamental difference in Hippo signaling between *Drosophila* and vertebrates (Bossuyt et al., 2013). Our present findings are consistent with a model in which AMOT retains YAP in a complex that is protected from LATS inhibition, but this AMOT-bound pool of YAP can then be mobilized by F-actin, promoting the release of YAP and its subsequent nuclear accumulation, resulting in increased transcription of its target genes (Figure 5I). In turn, this potential mechanism of YAP regulation may explain the still poorly understood mechanosensing role of YAP, and some seemingly contradictory results regarding AMOT function, as AMOT may act as a YAP inhibitor or facilitate YAP activation depending on the status of actin polymerization. These possibilities, as well as how the interplay between AMOT and LATS and the actin cytoskeleton (Adler et al., 2013; Chan et al., 2013; Dai et al., 2013; Hong, 2013; Paramasivam et al., 2011; Yi et al., 2013) regulates YAP will surely warrant further investigation.

A high rate of mutations in GPCRs and G proteins has been recently identified in melanoma (Kan et al., 2010; O'Hayre et al., 2013; Prickett et al., 2011). Strikingly, mutations in *GNAQ* and *GNA11* have been observed in the majority of uveal melanomas, 83% of blue naevi, 6% of cutaneous melanomas, and 59% of tumors arising in the meninges (Kusters-Vandevelde et al., 2010; Van Raamsdonk et al., 2009). Somatic mosaic mutations in *GNAQ* have been also recently identified in port-wine stains in infants and as the genetic alteration underlying Sturge-Weber syndrome (Shirley et al., 2013), while *GNA11* gain of function mutations causes autosomal dominant hypocalcemia (Nesbit et al., 2013). The growth promoting potential of *GNAQ* mutants requires the activation of a complex signaling network stimulating the expression of AP-1 regulated genes (Vaque et al., 2013). However, this signaling route may not yet be suitable for cancer treatment. Here, we show that activation of YAP represents a key molecular event downstream of *GNAQ* and *GNA11* in uveal melanoma. Moreover, recent efforts have exposed YAP as a suitable therapeutic target (Sudol et al., 2012). Liu-Chittenden *et al.* (Liu-Chittenden et al., 2012) screened a small-molecule library for compounds inhibiting the transcriptional activity of YAP *in vitro*. Among them, verteporfin, a benzoporphyrin derivative, is in clinical use as a photosensitizer in photocoagulation therapy for patients with wet age-related macular degeneration (Michels and Schmidt-Erfurth, 2001). Both YAP knock down and verteporfin treatment reduce uveal melanoma cell growth *in vitro* and tumor formation *in vivo*. In light of our observations, the successful use of photodynamic therapy (PDT) using verteporfin as a photosensitizer for the treatment of some patients with posterior uveal melanomas (Barbazetto et al., 2003; Soucek and Cihelkova, 2006) is very intriguing. It is presumed that the mechanism of action of PDT for uveal melanoma is damage to the tumor vasculature, but the pharmacological inhibition

of YAP by verteporfin may provide an unexpected alternative explanation for its therapeutic success in some patients. Indeed, although it is unclear whether VP may be also active in cancers driven by other tumor promoting genes, we can postulate that the transcriptional co-activator YAP may represent a suitable therapeutic target for the treatment of uveal melanoma and other human diseases that result from gain of function mutations in the *GNAQ* and *GNA11* oncogenes.

Experimental Procedures

Cell lines, culture procedures, and chemicals

Uveal melanoma OMM1.3, OMM1.5, Mel270 and 92.1 cells and cutaneous melanoma WM-266 and SK-mel-2 cells have been described elsewhere (Schmitt et al., 2007; Zuidervaart et al., 2005). Cells knock down for Trio and YAP and their corresponding controls were generated as described in the Supplemental experimental Procedures. Y-27632 (Tocris Cookson Inc., MO) (10μM) and Latrunculin A (Lat.A) (Tocris Cookson Inc., MO) (1μM) were used to treat uveal melanoma cells for 1h or 6h, followed by immunofluorescence, Western blot analysis and immunoprecipitation (IP) or qPCR, respectively. Verteporfin (VP) (CAS number: 129497-78-5; USP Reference Standards, Rockville, MD) was prepared as a stock solution in DMSO. See Supplemental Experimental Procedures.

siRNA and DNA constructs

All human siRNA sequences and providers, as well as DNA constructs are described in the Supplemental experimental Procedures.

Statistical analysis

All data analysis was performed using GraphPad Prism version 6 for Windows (GraphPad Software, CA). The data were analyzed by ANOVA test or t-test (* $p<0.05$, ** $p<0.01$, *** $p<0.001$).

Animal

All animal studies were approved by the Animal Care and User Committee (ACUC), National Institute of Dental and Craniofacial Research (NIDCR), in compliance with the "Guide for the Care and Use of Laboratory Animals." Animals were housed on 12-h light/dark cycles and received food, standard rodent chow, and water ad libitum in compliance with AAALAC guidelines. See also Supplemental experimental Procedures.

Human tumor xenografts and *in vivo* treatment with VP

Female NOD.Cg-*Prkdc*[scid]*Il2rg*[t][m1wjl]/SzJ mice 5 to 6 weeks of age and weighing 18 to 20g, were used in the study of tumor formation essentially as previously described (Vaque et al., 2013). The animals were monitored twice weekly for tumor development. Results of animal experiments were expressed as mean ± SEM of a total of 6 tumors analyzed. See Supplemental Experimental Procedures for the technical details and for the description of the treatment with VP (Liu-Chittenden et al., 2012).

Small GTPases activation, immunobloting, and posphoinositide (PI) turnover assays

RhoA and Rac1 activity was assessed by a modified method described previously (Patel et al., 2007). Western blots and posphoinositide (PI) turnover assays were performed as described previously (Vaque et al., 2013). See Supplemental experimental Procedures for antibody information and the technical details.

Immunorprecipitation and YAP-protein complex interaction and competition assays

See Supplemental experimental Procedures.

Clinical samples

Snap frozen uveal melanoma tissues were generously provided by Dr. James T. Handa and Dr. Shannath Merbs, Wilmer Eye Institute, Johns Hopkins School of Medicine; tissue was obtained from consenting patients in accordance with a study approved by the Institutional Review Board, at the Johns Hopkins School of Medicine. Normal skin samples were purchased from US Biomax and Biochain.

Immunofluorescence

See Supplemental experimental Procedures.

Luciferase Assays

HEK293 cells were co-transfected with TEAD4-Gal4 (0.5μg/ml), Gal4-luc (0.5μg/ml) and pRLNull (1μg/ml) in 24-well plates overnight to the detection of the luciferase activity, using a Dual-Glo Luciferase Assay Kit (Promega, WI) and a Microtiter plate luminometer (Dynex Tech., VA).

Immunohistochemistry

See Supplemental experimental Procedures.

Growth in Soft Agar

Cells were mixed at a concentration of 2,500 cells/0.2 ml of medium, and 0.2% agar (Lonza, MD). The cells in 0.2% agar were plated over 0.2 ml of medium, 1% agar that had been allowed to harden in a 96-well dish. Cells were fed 50μl of medium every 4 days. In the VP treatment assay, VP was added in the medium with final concentration 1μM.

Nuclear and Cytoplasm Extraction

Follow the instructions of NE-PER Nuclear and Cytoplasmic Extraction Reagents (Thermo Scientific, CO).

Supplementary Material

Refer to Web version on PubMed Central for supplementary material.

Acknowledgments

References

Adler JJ, Johnson DE, Heller BL, Bringman LR, Ranahan WP, Conwell MD, Sun Y, Hudmon A, Wells CD. Serum deprivation inhibits the transcriptional co-activator YAP and cell growth via phosphorylation of the 130-kDa isoform of Angiomotin by the LATS1/2 protein kinases. Proceedings of the National Academy of Sciences of the United States of America. 2013; 110:17368–17373. [PubMed: 24101513]

Aragona M, Panciera T, Manfrin A, Giulitti S, Michielin F, Elvassore N, Dupont S, Piccolo S. A Mechanical Checkpoint Controls Multicellular Growth through YAP/TAZ Regulation by Actin-Processing Factors. Cell. 2013; 154:1047–1059. [PubMed: 23954413]

Bar-Sagi D, Hall A. Ras and Rho GTPases: a family reunion. Cell. 2000; 103:227–238. [PubMed: 11057896]

Barbazetto IA, Lee TC, Rollins IS, Chang S, Abramson DH. Treatment of choroidal melanoma using photodynamic therapy. Am J Ophthalmol. 2003; 135:898–899. [PubMed: 12788137]

Berman DM, Wilkie TM, Gilman AG. GAIP and RGS4 are GTPase-activating proteins for the G(i) subfamily of G protein alpha subunits. Cell. 1996; 86:445–452. [PubMed: 8756726]

Bernard O. Lim kinases, regulators of actin dynamics. Int J Biochem Cell Biol. 2007; 39:1071–1076. [PubMed: 17188549]

Bossuyt W, Chen CL, Chen Q, Sudol M, McNeill H, Pan D, Kopp A, Halder G. An evolutionary shift in the regulation of the Hippo pathway between mice and flies. Oncogene. 2013

Camargo FD, Gokhale S, Johnnidis JB, Fu D, Bell GW, Jaenisch R, Brummelkamp TR. YAP1 increases organ size and expands undifferentiated progenitor cells. Current Biology. 2007; 17:2054–2060. [PubMed: 17980593]

Castellano M, Pollock PM, Walters MK, Sparrow LE, Down LM, Gabrielli BG, Parsons PG, Hayward NK. CDKN2A/p16 is inactivated in most melanoma cell lines. Cancer Res. 1997; 57:4868–4875. [PubMed: 9354451]

Chan SW, Lim CJ, Chong YF, Pobbati AV, Huang C, Hong W. Hippo pathway-independent restriction of TAZ and YAP by angiomotin. The Journal of Biological Chemistry. 2011; 286:7018–7026. [PubMed: 21224387]

Chan SW, Lim CJ, Guo F, Tan I, Leung T, Hong W. Actin-binding and Cell Proliferation Activities of Angiomotin Family Members Are Regulated by Hippo Pathway-mediated Phosphorylation. The Journal of Biological Chemistry. 2013; 288:37296–37307. [PubMed: 24225952]

Dai X, She P, Chi F, Feng Y, Liu H, Jin D, Zhao Y, Guo X, Jiang D, Guan KL, et al. Phosphorylation of angiomotin by Lats1/2 kinases inhibits F-actin binding, cell migration, and angiogenesis. The Journal of Biological Chemistry. 2013; 288:34041–34051. [PubMed: 24106267]

Dong J, Feldmann G, Huang J, Wu S, Zhang N, Comerford SA, Gayyed MF, Anders RA, Maitra A, Pan D. Elucidation of a universal size-control mechanism in Drosophila and mammals. Cell. 2007; 130:1120–1133. [PubMed: 17889654]

Dupont S, Morsut L, Aragona M, Enzo E, Giulitti S, Cordenonsi M, Zanconato F, Le Digabel J, Forcato M, Bicciato S, et al. Role of YAP/TAZ in mechanotransduction. Nature. 2011; 474:179–183. [PubMed: 21654799]

Griner EM, Kazanietz MG. Protein kinase C and other diacylglycerol effectors in cancer. Nature reviews Cancer. 2007; 7:281–294. [PubMed: 17384583]

Halder G, Dupont S, Piccolo S. Transduction of mechanical and cytoskeletal cues by YAP and TAZ. Nat Rev Mol Cell Biol. 2012; 13:591–600. [PubMed: 22895435]

Hong W. Angiomotin'g YAP into the nucleus for cell proliferation and cancer development. Science Signaling. 2013; 6:pe27. [PubMed: 24003252]

Hubbard KB, Hepler JR. Cell signalling diversity of the Gqalpha family of heterotrimeric G proteins. Cellular Signalling. 2006; 18:135–150. [PubMed: 16182515]

Johnson R, Halder G. The two faces of Hippo: targeting the Hippo pathway for regenerative medicine and cancer treatment. Nature reviews Drug Discovery. 2014; 13:63–79. [PubMed: 24336504]

Kan Z, Jaiswal BS, Stinson J, Janakiraman V, Bhatt D, Stern HM, Yue P, Haverty PM, Bourgon R, Zheng J, et al. Diverse somatic mutation patterns and pathway alterations in human cancers. Nature. 2010; 466:869–873. [PubMed: 20668451]

Kusters-Vandevelde HV, Klaasen A, Kusters B, Groenen PJ, van Engen-van Grunsven IA, van Dijk MR, Reifenberger G, Wesseling P, Blokx WA. Activating mutations of the GNAQ gene: a frequent event in primary melanocytic neoplasms of the central nervous system. Acta Neuropathol. 2010; 119:317–323. [PubMed: 19936769]

Liu-Chittenden Y, Huang B, Shim JS, Chen Q, Lee SJ, Anders RA, Liu JO, Pan DJ. Genetic and pharmacological disruption of the TEAD-YAP complex suppresses the oncogenic activity of YAP. Genes & Development. 2012; 26:1300–1305. [PubMed: 22677547]

Matsui Y, Lai ZC. Mutual regulation between Hippo signaling and actin cytoskeleton. Protein & Cell. 2013; 4:904–910. [PubMed: 24248471]

Michels S, Schmidt-Erfurth U. Photodynamic therapy with verteporfin: a new treatment in ophthalmology. Semin Ophthalmol. 2001; 16:201–206. [PubMed: 15513441]

Mo JS, Yu FX, Gong R, Brown JH, Guan KL. Regulation of the Hippo-YAP pathway by protease-activated receptors (PARs). Genes & Development. 2012; 26:2138–2143. [PubMed: 22972936]

Mohseni M, Sun J, Lau A, Curtis S, Goldsmith J, Fox VL, Wei C, Frazier M, Samson O, Wong KK, et al. A genetic screen identifies an LKB1-MARK signalling axis controlling the Hippo-YAP pathway. Nature Cell Biology. 2014; 16:108–117. [PubMed: 24362629]

Nesbit MA, Hannan FM, Howles SA, Babinsky VN, Head RA, Cranston T, Rust N, Hobbs MR, Heath H 3rd, Thakker RV. Mutations affecting G-protein subunit alpha11 in hypercalcemia and hypocalcemia. N Engl J Med. 2013; 368:2476–2486. [PubMed: 23802516]

O'Hayre M, Vazquez-Prado J, Kufareva I, Stawiski EW, Handel TM, Seshagiri S, Gutkind JS. The emerging mutational landscape of G proteins and G-protein-coupled receptors in cancer. Nature reviews Cancer. 2013; 13:412–424.

Oka T, Schmitt AP, Sudol M. Opposing roles of angiomotin-like-1 and zona occludens-2 on pro-apoptotic function of YAP. Oncogene. 2012; 31:128–134. [PubMed: 21685940]

Pan DJ. The Hippo Signaling Pathway in Development and Cancer. Developmental Cell. 2010; 19:491–505. [PubMed: 20951342]

Paramasivam M, Sarkeshik A, Yates JR 3rd, Fernandes MJ, McCollum D. Angiomotin family proteins are novel activators of the LATS2 kinase tumor suppressor. Molecular Biology of the Cell. 2011; 22:3725–3733. [PubMed: 21832154]

Pollard TD, Cooper JA. Actin, a central player in cell shape and movement. Science. 2009; 326:1208–1212. [PubMed: 19965462]

Prickett TD, Wei X, Cardenas-Navia I, Teer JK, Lin JC, Walia V, Gartner J, Jiang J, Cherukuri PF, Molinolo A, et al. Exon capture analysis of G protein-coupled receptors identifies activating mutations in GRM3 in melanoma. Nat Genet. 2011; 43:1119–1126. [PubMed: 21946352]

Radu M, Semenova G, Kosoff R, Chernoff J. PAK signalling during the development and progression of cancer. Nature reviews Cancer. 2014; 14:13–25. [PubMed: 24505617]

Ramos A, Camargo FD. The Hippo signaling pathway and stem cell biology. Trends in Cell Biology. 2012; 22:339–346. [PubMed: 22658639]

Schlegelmilch K, Mohseni M, Kirak O, Pruszak J, Rodriguez JR, Zhou D, Kreger BT, Vasioukhin V, Avruch J, Brummelkamp TR, et al. Yap1 acts downstream of alpha-catenin to control epidermal proliferation. Cell. 2011; 144:782–795. [PubMed: 21376238]

Schmitt CJ, Franke WW, Goerdt S, Falkowska-Hansen B, Rickelt S, Peitsch WK. Homo- and heterotypic cell contacts in malignant melanoma cells and desmoglein 2 as a novel solitary surface glycoprotein. J Invest Dermatol. 2007; 127:2191–2206. [PubMed: 17495963]

Shirley MD, Tang H, Gallione CJ, Baugher JD, Frelin LP, Cohen B, North PE, Marchuk DA, Comi AM, Pevsner J. Sturge-Weber syndrome and port-wine stains caused by somatic mutation in GNAQ. N Engl J Med. 2013; 368:1971–1979. [PubMed: 23656586]

Soucek P, Cihelkova I. Photodynamic therapy with verteporfin in subfoveal amelanotic choroidal melanoma (A controlled case). Neuro Endocrinol Lett. 2006; 27:145–148. [PubMed: 16648785]

Sudol M. YAP1 oncogene and its eight isoforms. Oncogene. 2013; 32:3922. [PubMed: 23160371]

Sudol M, Bork P, Einbond A, Kastury K, Druck T, Negrini M, Huebner K, Lehman D. Characterization of the mammalian YAP (Yes-associated protein) gene and its role in defining a novel protein module, the WW domain. The Journal of Biological Chemistry. 1995; 270:14733–14741. [PubMed: 7782338]

Sudol M, Shields DC, Farooq A. Structures of YAP protein domains reveal promising targets for development of new cancer drugs. Semin Cell Dev Biol. 2012; 23:827–833. [PubMed: 22609812]

van der Velden PA, Metzelaar-Blok JA, Bergman W, Monique H, Hurks H, Frants RR, Gruis NA, Jager MJ. Promoter hypermethylation: a common cause of reduced p16(INK4a) expression in uveal melanoma. Cancer Res. 2001; 61:5303–5306. [PubMed: 11431374]

Van Raamsdonk CD, Bezrookove V, Green G, Bauer J, Gaugler L, O'Brien JM, Simpson EM, Barsh GS, Bastian BC. Frequent somatic mutations of GNAQ in uveal melanoma and blue naevi. Nature. 2009; 457:599–602. [PubMed: 19078957]

Van Raamsdonk CD, Griewank KG, Crosby MB, Garrido MC, Vemula S, Wiesner T, Obenauf AC, Wackernagel W, Green G, Bouvier N, et al. Mutations in GNA11 in uveal melanoma. N Engl J Med. 2010; 363:2191–2199. [PubMed: 21083380]

Vaque JP, Dorsam RT, Feng XD, Iglesias-Bartolome R, Forsthoefel DJ, Chen QM, Debant A, Seeger MA, Ksander BR, Teramoto H, et al. A Genome-wide RNAi Screen Reveals a Trio-Regulated Rho GTPase Circuitry Transducing Mitogenic Signals Initiated by G Protein-Coupled Receptors. Molecular Cell. 2013; 49:94–108. [PubMed: 23177739]

Vitale-Cross L, Amornphimoltham P, Fisher G, Molinolo AA, Gutkind JS. Conditional expression of K-ras in an epithelial compartment that includes the stem cells is sufficient to promote squamous cell carcinogenesis. Cancer Res. 2004; 64:8804–8807. [PubMed: 15604235]

Wang W, Li X, Huang J, Feng L, Dolinta KG, Chen J. Defining the protein-protein interaction network of the human hippo pathway. Molecular & Cellular Proteomics : MCP. 2014; 13:119–131. [PubMed: 24126142]

Yi C, Shen Z, Stemmer-Rachamimov A, Dawany N, Troutman S, Showe LC, Liu Q, Shimono A, Sudol M, Holmgren L, et al. The p130 isoform of angiomotin is required for Yap-mediated hepatic epithelial cell proliferation and tumorigenesis. Science Signaling. 2013; 6:ra77. [PubMed: 24003254]

Yin F, Yu J, Zheng Y, Chen Q, Zhang N, Pan D. Spatial organization of Hippo signaling at the plasma membrane mediated by the tumor suppressor Merlin/NF2. Cell. 2013; 154:1342–1355. [PubMed: 24012335]

Yu FX, Zhao B, Panupinthu N, Jewell JL, Lian I, Wang LH, Zhao JG, Yuan HX, Tumaneng K, Li HR, et al. Regulation of the Hippo-YAP Pathway by G-Protein-Coupled Receptor Signaling. Cell. 2012; 150:780–791. [PubMed: 22863277]

Zaidi MR, Davis S, Noonan FP, Graff-Cherry C, Hawley TS, Walker RL, Feigenbaum L, Fuchs E, Lyakh L, Young HA, et al. Interferon-gamma links ultraviolet radiation to melanomagenesis in mice. Nature. 2011; 469:548–553. [PubMed: 21248750]

Zhao B, Li L, Lei Q, Guan KL. The Hippo-YAP pathway in organ size control and tumorigenesis: an updated version. Genes & development. 2010; 24:862–874. [PubMed: 20439427]

Zhao B, Li L, Lu Q, Wang LH, Liu CY, Lei Q, Guan KL. Angiomotin is a novel Hippo pathway component that inhibits YAP oncoprotein. Genes & Development. 2011; 25:51–63. [PubMed: 21205866]

Zhao B, Wei X, Li W, Udan RS, Yang Q, Kim J, Xie J, Ikenoue T, Yu J, Li L, et al. Inactivation of YAP oncoprotein by the Hippo pathway is involved in cell contact inhibition and tissue growth control. Genes & development. 2007; 21:2747–2761. [PubMed: 17974916]

Zuidervaart W, van Nieuwpoort F, Stark M, Dijkman R, Packer L, Borgstein AM, Pavey S, van der Velden P, Out C, Jager MJ, et al. Activation of the MAPK pathway is a common event in uveal

melanomas although it rarely occurs through mutation of BRAF or RAS. Br J Cancer. 2005; 92:2032–2038. [PubMed: 15928660]

Highlights

- The *GNAQ* oncogene stimulates the transcriptional co-activator YAP in uveal melanoma

- A Hippo- and PLCβ-independent Rho GTPase signaling circuitry links *GNAQ* to YAP

- YAP is essential for *GNAQ*-induced uveal melanoma cell proliferation

- YAP represents a novel therapeutic target for melanomas harboring *GNAQ* mutations

Significance

Uveal melanoma is the most frequent ocular malignancy in adults, for which no effective systemic therapies are currently available. Recent findings revealed that activating mutations in *GNAQ* and *GNA11*, encoding members of the Gαq family of G protein α subunits, drive uveal melanoma oncogenesis. Here we report that *GNAQ* stimulates the transcriptional co-activator YAP in human uveal melanoma cells and *GNAQ*-induced cancer mouse models. At the molecular level, Gαq activates YAP by acting on a Hippo-independent signaling network initiated by actin polymerization. Ultimately, YAP is essential for uveal melanoma cell proliferation, thereby rendering it sensitive to clinically-relevant small molecule YAP inhibitors. Hence, this cancer vulnerability can be exploited for the development of new precision molecular therapies for *GNAQ*-driven human malignancies.
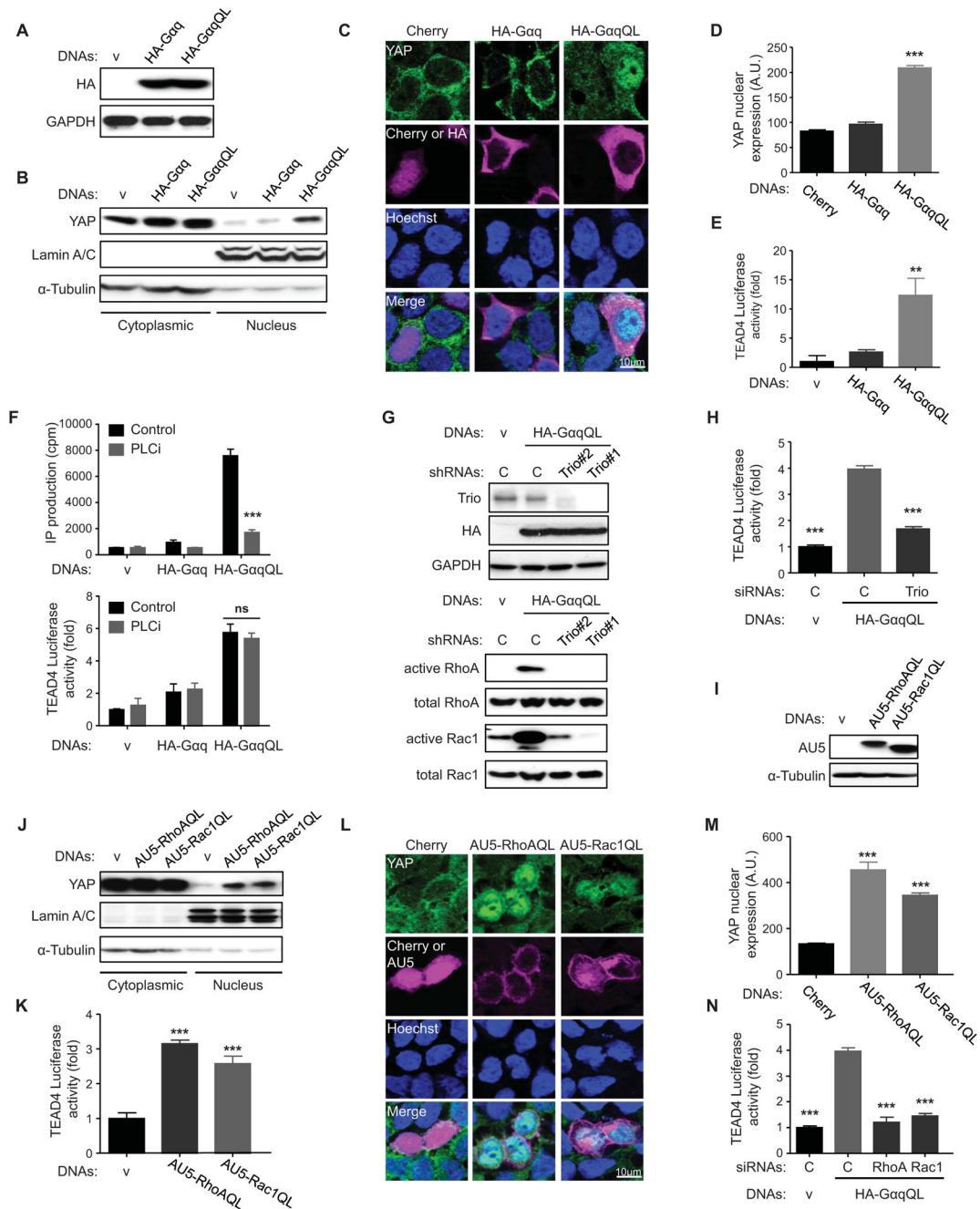
Figure 1. Activating mutations in Gαq (GαqQL) induces YAP nuclear translocation and YAP-Dependent Transcription activation through Trio and Trio dependent Rho-GTPases

(A) Western blots show HA-Gαq and HA-GαqQL expression in HEK293 cells transfected with HA-Gαq or HA-GαqQL expression vectors (DNAs), using endogenous GAPDH as a loading control. (B) Western blot shows YAP expression levels in the nuclear fraction; enrichment for Lamin A/C and α-Tubulin served as nuclear and cytoplasmic markers respectively. (C and D) Immunofluorescence shows that transfected GαqQL induces YAP nuclear translocation, but not Gαq or mCherry. (C) Endogenous YAP (green) was detected by immunofluorescence along with Hoechst for nuclear DNA (blue) and HA staining

(violet) or mCherry (violet, as control). (D) Nuclear YAP in HA-positive and mCherry-positive cells was quantified with Image-J and represented as arbitrary units in the indicated cell populations (mean ± SEM, n = 50–100 cells). (E) HEK293 cells were cotransfected with HA-Gαq or HA-GαqQL and Gal4-TEAD4, 5×UAS-Luc and Renilla-Luc DNAs followed by luciferase assay (mean ± SEM, n = 3). (F) HEK293 cells were transfected with HA-Gαq or HA-GαqQL, followed by posphoinositide (PI) turnover assays (mean ± SEM, n = 6) (upper panel) or cotransfected with Gal4-TEAD4, 5×UAS-Luc and Renilla-Luc DNAs, followed by PLCi treatment (1 hr) and luciferase assay (mean ± SEM, n = 3) (lower panel). (G) Transfected HA-GαqQL or vector into shRNA-control, shRNA-Trio#1 and shRNA–Trio#2 HEK293 cells, followed by the indicated Western blot analysis (upper panel) or by RhoA and Rac1 small GTPases activation assays (lower panels). (H) HEK293 cells were cotransfected with siRNA Trio or control and HA-GαqQL or vector and Gal4-TEAD4, 5×UAS-Luc and Renilla-Luc DNAs, followed by luciferase assay (mean ± SEM, n = 6). (I) Western blot show AU5-RhoAQL and AU5-Rac1QL expression in HEK293 cells transfected with the corresponding expression plasmids. (J) Western blots show that both RhoAQL and Rac1QL can induce YAP accumulation in the nuclear fraction, using enrichment in Lamin A/C and α-Tubulin as nuclear and cytoplasmic markers respectively. (K) HEK293 cells were cotransfected with AU5-RhoAQL or AU5-Rac1QL and Gal4-TEAD4, 5×UAS-Luc and Renilla-Luc DNAs, followed by luciferase assays (mean ± SEM, n = 6). (L and M) Immunofluorescence assay and nuclear YAP quantification, using the procedure described in 1C in the indicated transfected cells (mean ± SEM, n = 50–100 cells). (N) HEK293 cells were cotransfected with siRNAs RhoA, Rac1 or control and HA-GαqQL or vector and Gal4-TEAD4, 5×UAS-Luc and Renilla-Luc DNAs, followed by luciferase assay, as above (mean ± SEM, n = 6). See also Figure S1.
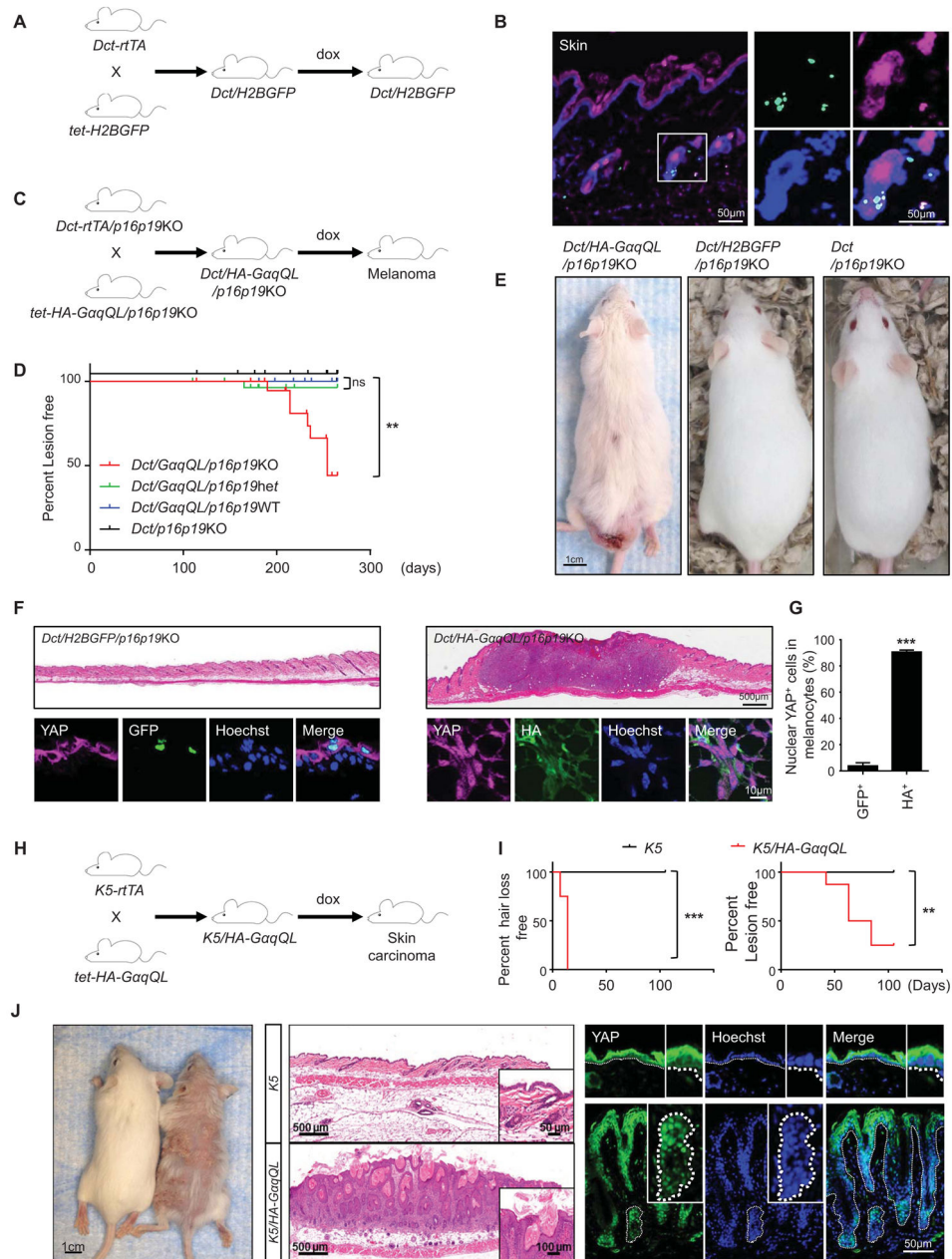
Figure 2. Conditional expression of the GαqQL promotes melanoma or skin carcinoma formation and YAP activation *in vivo*

(A) *Dct-rtTA* mice were bred with *tet-H2BGFP* transgenic mice to produce inducible *Dct/H2BGFP* double transgenic mice, which express GFP exclusively in melanocytes, when fed with doxycycline food (dox). (B) *Dct/H2BGFP* mice show tight regulation GFP expression in skin melanocytes (as showed in Zaidi et al., 2011) (C) *Dct-rtTA/p16p19*KO mice were bred with *tet-HA-GαqQL/p16p19*KO mice to produce inducible *Dct/HA-GαqQL/p16p19*KO mice, which expressed HA-GαqQL exclusively in melanocytes, when fed with doxycycline food (dox). (D) Percentage of mice developing cutaneous lesions of melanocytic origin after feeding with doxycycline food. (E) Example of Dct/HA-GαqQL/p16p19KO mice

developing lesions in the skin. (F) Histology shows *Dct/HA-GαqQL/p16p19*KO mouse with cutaneous melanoma (upper right panel). Immunofluorescence assay of frozen tissues shows that HA-GαqQL (green) positive cells display YAP (violet) nuclear translocation using Hoechst for DNA staining (blue) (right lower panel). Normal skin from *Dct/H2BGFP* mouse stained with GFP (green) instead of HA as control (left lower panel) shows cytoplasmic YAP. (G) Quantification of percent nuclear YAP positive cells in GFP or HA positive cells (GFP+ and HA+, respectively). (H) *K5-rtTA* mice were bred with *tet-O-HA-GαqQL* mice to produce inducible *K5/HA-GαqQL* mice, which express HA-GαqQL exclusively in basal epithelial cells (Vitale-Cross et al., 2004), when fed with doxycycline food (dox). (I) *K5/HA-GαqQL* mice developed rapid hair loss within days (left), and exhibited multiple tumor lesions on the skin (right). (J) Histology showed that these *K5/HA-GαqQL* mice developed skin carcinoma (middle lower panel). Immunofluorescence assays in frozen tissues show that *K5/HA-GαqQL* mice exhibit YAP (green) nuclear translocation, using Hoechst to stain nuclear DNA (blue) (right lower panels). See also Figure S2.
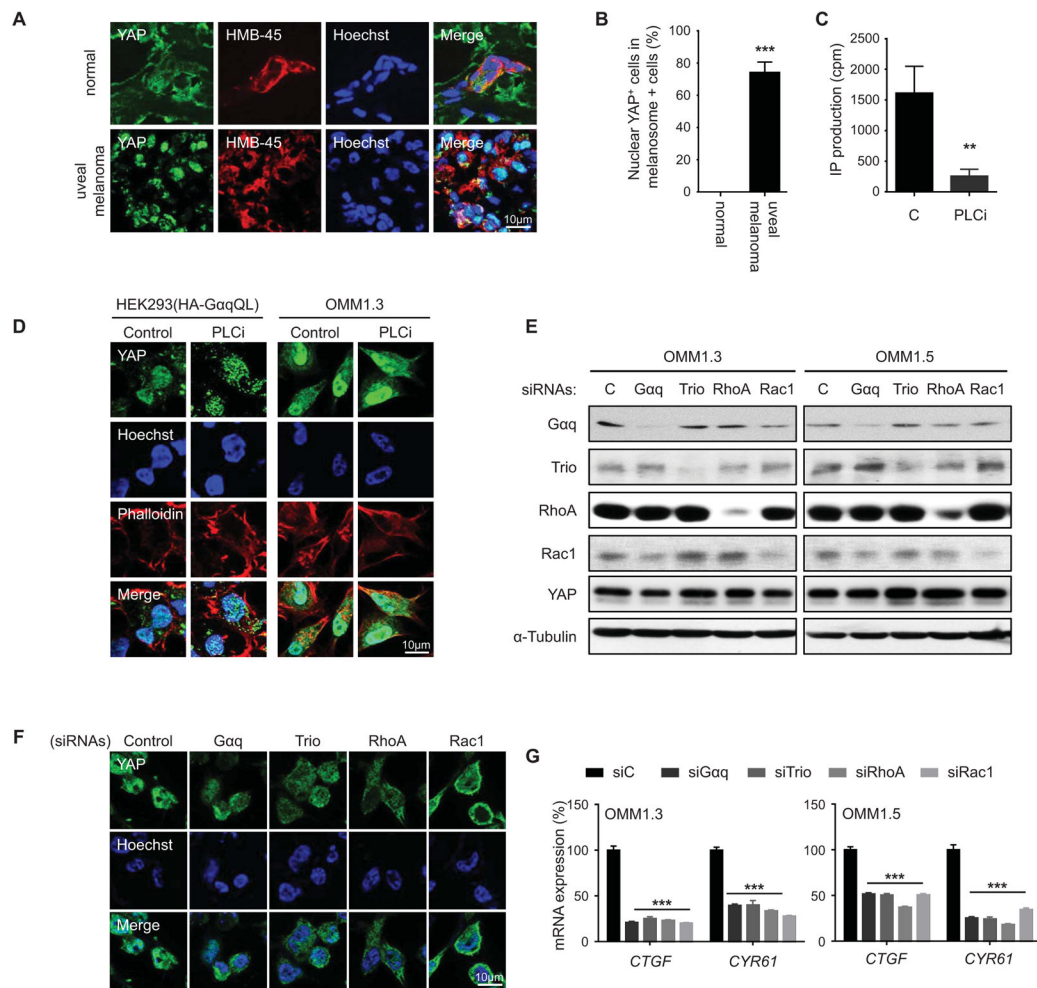
Figure 3. Trio and a network of Rho-GTPases mediate YAP activation in uveal melanoma cells harboring *GNAQ* mutations

(A) Immunofluorescence assays using frozen tissues from clinical uveal melanoma specimens (n = 6) showed HMB-45-positive cells (red) with nuclear YAP (green), using Hoeschst to stain nuclear DNA (blue), using as control HMB-45 staining to identify the resident melanocytes in normal tissues (n = 3). (B) Quantification of percent nuclear YAP positive cells in melanosome positive cells. (C) PLCi inhibits the hydrolysis of phosphoinositides in OMIM1.3 uveal melanoma cells as judged by PI turnover assays. (D) HEK293 cells transfected with GαqQL expression vectors and OMM1.3 uveal melanoma cells exhibited nuclear YAP by immunofluorescence (green), which was insensitive to PLC inhibition (PLCi), using Hoeschst and phalloidin to stain nuclear DNA (blue) and cytoplasmic polymerized actin (red), respectively. (E) Western blot analysis documents knock down using siRNAs in two uveal melanoma cell lines. (F) OMM1.3 uveal melanoma transfected with siRNA-control show cells with YAP (green) nuclear staining, while cells transfected with the indicated siRNAs show YAP mainly localized to the cytoplasm. Hoechst stains nuclear DNA (blue). (G) siRNAs knockdown of Gαq, Trio, RhoA or Rac1 diminish the expression of endogenous YAP-regulated genes (*CTGF* and *CYR61*) in OMM1.3 and OMM1.5 uveal melanoma cells (mean ± SEM, n = 3).
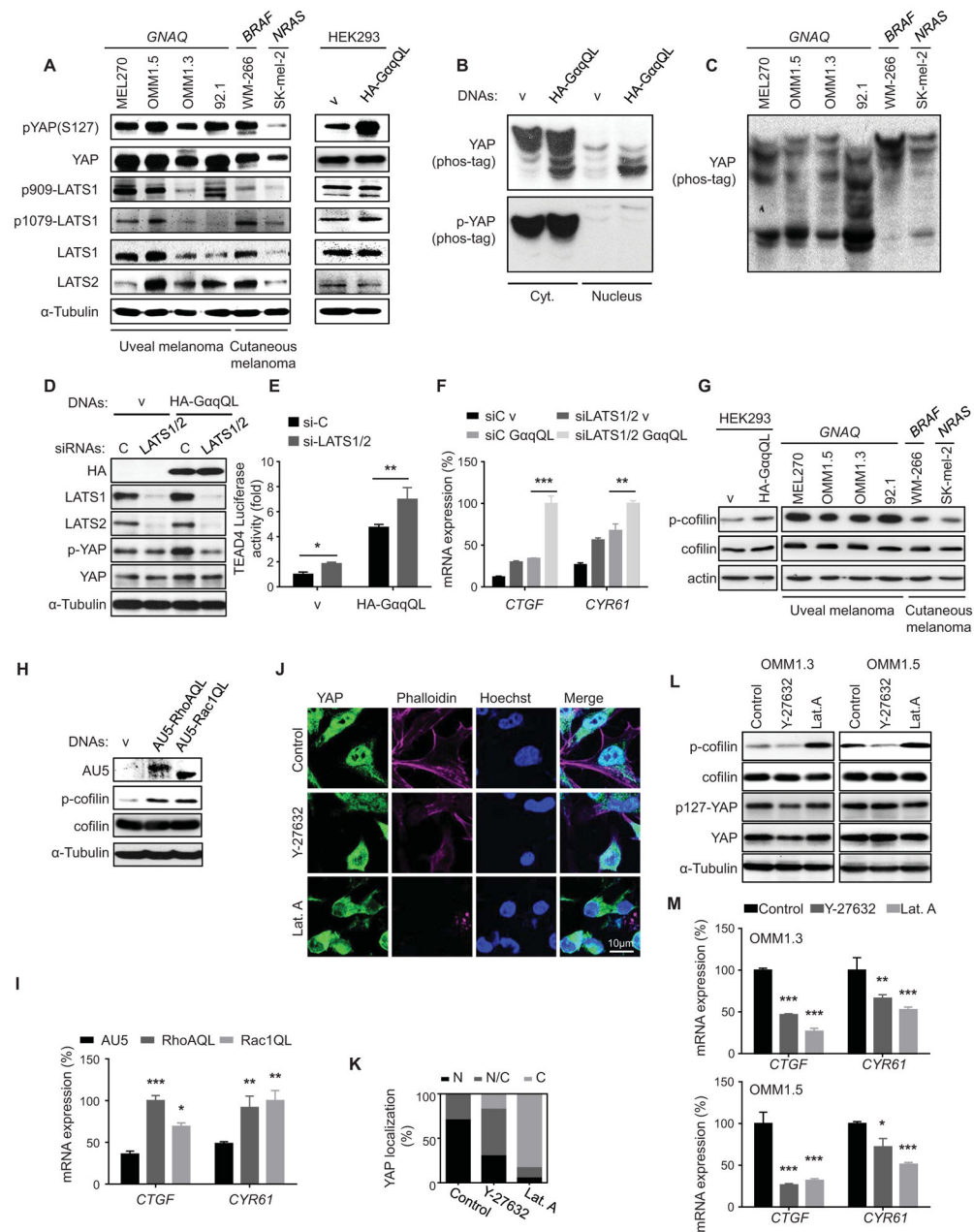
Figure 4. *GNAQ* **oncogenic signaling induces YAP nuclear translocation and YAP-dependent transcription activation through Rho-GTPases and actin remodeling**
(A) Western blots show expression of total and phosphorylated (serine 127) YAP and LATS1 and LATS2 in uveal and cutaneous melanoma cells, the latter expressing *BRAF* and *NRAS* oncogenes, as indicated, as well as in HEK293 cells expressing GαqQL or vector (v) as controls. (B and C) Cell lysates were subjected to immunoblotting with the indicated antibodies. Gels containing phos-tag were employed to assess YAP phosphorylation status. Dephosphorylated YAP was reflected by the faster migration of YAP. (B) Phosphorylated YAP (p-YAP and slower mobility forms) and dephosphorylated YAP in the cytosolic (Cyt.) and nuclear (Nucleus) fractions of HEK293 cells transfected with GαqQL or vector control. (C) Phosphorylated YAP (slower mobility forms) in uveal and cutaneous melanoma cells

expressing the indicated oncogenes. (D) HEK293 cells were cotransfected with siRNA LATS1 and LATS2 or control and HA-GαqQL or vector DNAs, followed by the indicated Western blot analysis for HA-Gαq, LATS1, LATS2, p(127)-YAP, YAP and α-Tubulin as a loading control. (E) Similarly, cells were also transfected with Gal4-TEAD4, 5×UAS-Luc and Renilla-Luc DNAs, followed by luciferase assay (mean ± SEM, n = 3). (F) Cells were also studied by qPCR to assess the expression levels of YAP-regulated genes (*CTGF* and *CYR61*) (mean ± SEM, n = 3). (G) Levels of cofilin and phospho-cofilin (p-cofilin) in HEK293 cells expressing GαqQL or vector control, as well as in the indicated uveal and cutaneous melanoma cells. (H) Accumulation of phosphorylated cofilin in HEK293 cells expressing RhoAQL or Rac1QL. (I) Expression of YAP regulated genes (*CTGF* and *CYR61*) in HEK293 cells expressing RhoAQL or Rac1QL (mean ± SEM, n = 3). (J) OMM1.3 uveal melanoma cells treated with Y-27632 or Latrunculin A (Lat.A), following with Immunofluorescence assay, YAP (green), Hoechst stains nuclear DNA (blue) and phalloidin stains F-actin (violet). (K) Proportion of cells displaying preferential nuclear (N), nuclear and cytoplasmic (N/C), or cytoplasmic (C) YAP location (left panel; N=50–100 cells). (L) Y-27632 or Lat.A treatments were followed by Western blot analysis for p-cofilin, cofilin, p127-YAP, YAP, and α-Tubulin as a loading control. (M) Impact of Y-27632 and Lat.A treatments on the expression of endogenous YAP-regulated genes (*CTGF* and *CYR61*) in OMM1.3 and OMM1.5 uveal melanoma cells (mean ± SEM, n = 3). See also Figure S3.
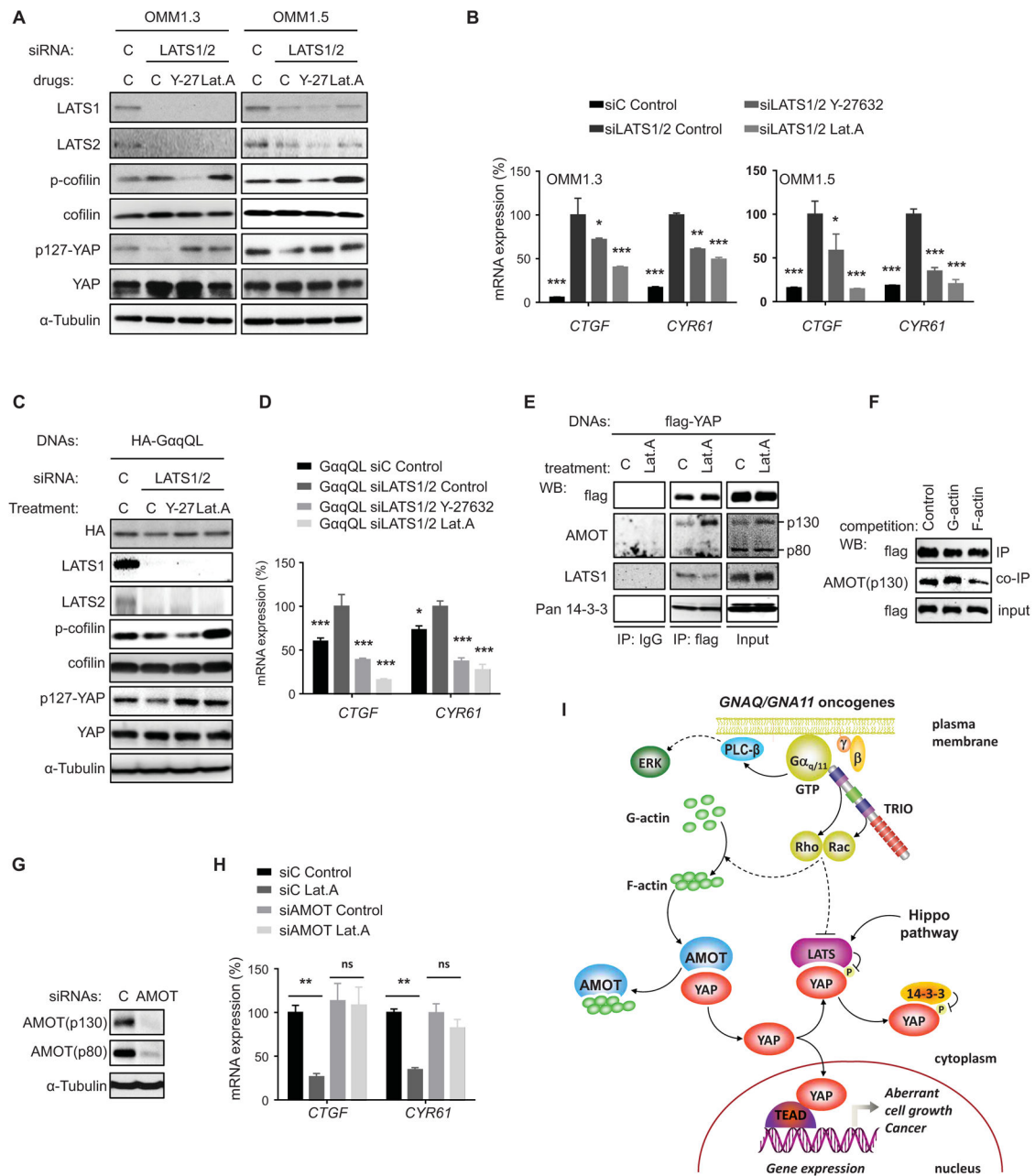
Figure 5. Actin remodeling results in Hippo-independent activation of YAP downstream from *GNAQ* oncogenic signaling
(A) OMM1.3 and OMM1.5 cells were transfected with siRNAs for LATS1 and LATS2 and treated with control diluent or Y-27632 and Lat.A, followed by Western blot analysis for LATS1, LATS2, p-cofilin, cofilin, p127-YAP, YAP and α-Tubulin as a loading control. (B) Similarly, cells were also followed by qPCR to analyze the expression of YAP-regulated genes (*CTGF* and *CYR61*) (mean ± SEM, n = 3). (C) HEK293 cells were cotransfected with siRNA LATS1 and LATS2 and HA-GαqQL, and treated with Y-27632 or Lat.A followed by the indicated Western blot analysis for HA-GαqQL, LATS1, LATS2, p-cofilin, cofilin, p127-YAP, YAP and α-Tubulin as a loading control. (D) Cells were also followed by qPCR

to assess the expression levels of YAP-regulated genes (*CTGF* and *CYR61*) (mean ± SEM, n = 3). (E) OMM1.3 cells expressing flag-tagged YAP treated with Lat.A or control, were lysed and followed by anti-flag and control (IgG) immunoprecipitation (IP) and Western blot analysis for flag-YAP, AMOT, LATS1, and 14-3-3 present in the immuneprecipitates, using the input lysate as control. (F) Anti-flag immunoprecipitates (IP) from HEK293 cells expressing flag-YAP were exposed to G-actin or F-actin, washed, and analyzed by Western blot for flag-YAP and associated endogenous AMOT. (G) OMM1.3 cells were transfected with siRNA for AMOT, followed by the indicated Western blot analysis for AMOT (recognizing both p130 and p80 forms) and α-Tubulin as a loading control. (H) OMM1.3 were transfected with siRNA AMOT or siRNA control, followed by Lat.A treatment or control, and the expression of YAP-regulated genes (*CTGF* and *CYR61*) was determined by qPCR. (I) Schematic representation of Hippo-dependent and –independent pathways resulting in YAP activation by the *GNAQ* oncogene in uveal melanoma. Gαq protein stimulates YAP through a RhoA and Rac1 regulated signaling circuitry initiated by the activation of TRIO, a Rho-GEF activating these GTPases, independently of the best-known stimulation of second messengers through PLC-β. In turn, RhoA activates ROCK and Rac1 stimulates PAK proteins, which converge in the activation of LIMK that phosphorylates and inactivates the actin severing protein cofilin, resulting in actin polymerization and F-actin accumulation (not depicted for simplicity, dotted line). F–actin may then bind AMOT, displacing YAP, which translocates to the nucleus and initiates gene expression. Free YAP can also bind to LATS, which phosphorylates and inactivates YAP upon the cytosolic sequestration of phospho-YAP by 14-3-3 proteins or by promoting its proteosomal degradation (the latter not depicted), as part of a canonical Hippo-dependent pathway restraining YAP function. How Rho GTPases regulate LATS function is not fully understood (dotted line). It is expected that in the presence of *GNAQ* oncogenes, LATS reduced activity acts in a coordinated function with the likely dominant F-actin-mediated stimulation of YAP to promote YAP stabilization and nuclear translocation, ultimately resulting in the expression of YAP-regulated growth-promoting genes. See text for details.
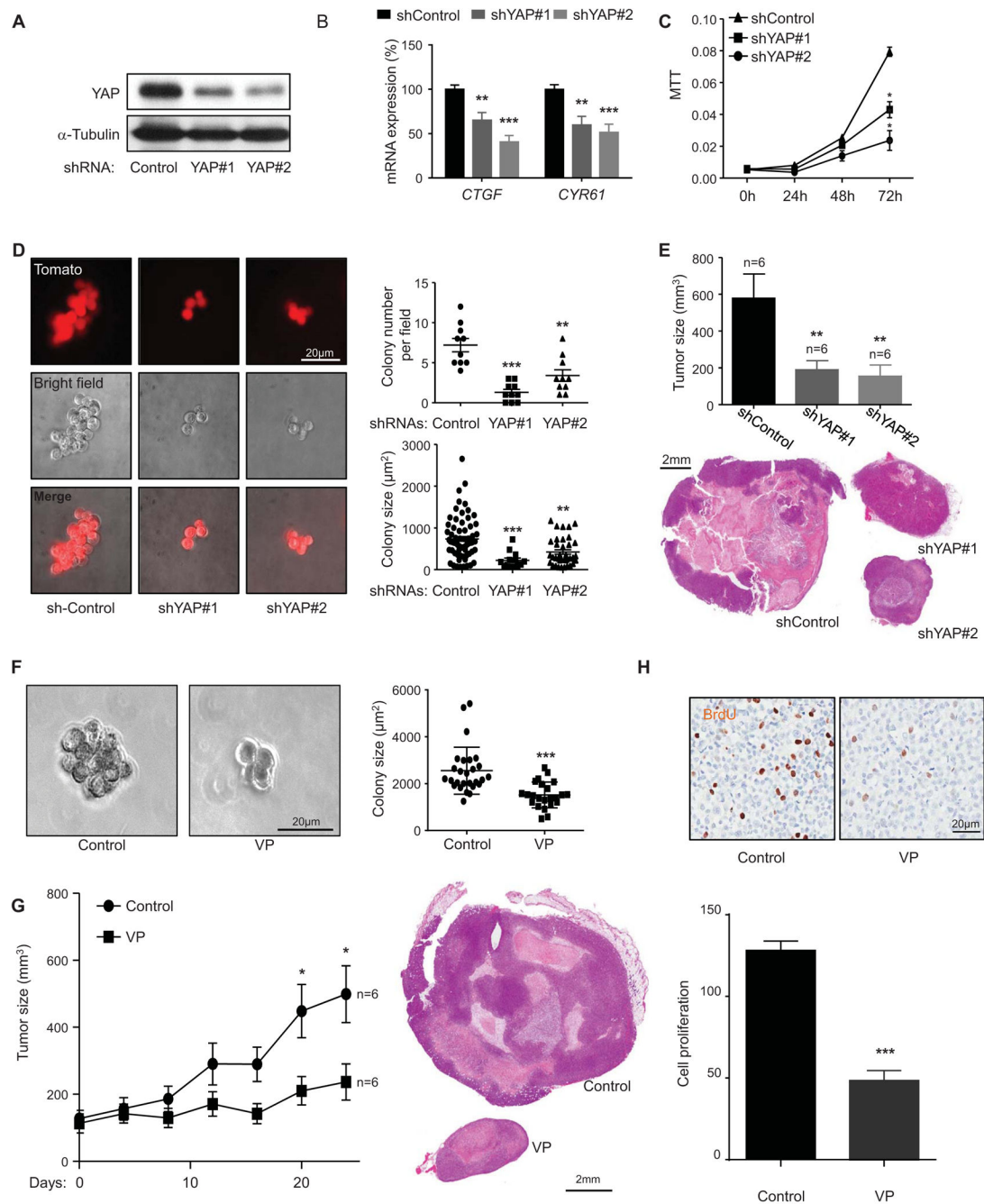
Figure 6. YAP represents a therapeutic target in uveal melanoma

(A) Western blot show YAP knockdown by doxycycline inducible shRNAs (YAP#1 and YAP#2) in OMM1.3 uveal melanoma cells. (B) Impact of shRNAs knocking down YAP on the expression of endogenous YAP-regulated genes (*CTGF* and *CYR61*) in OMM1.3 uveal melanoma cells (mean ± SEM, n = 5). (C) Effect of shRNAs knock down of YAP in OMM1.3 uveal melanoma cells proliferation (mean ± SEM, n = 3). (D) OMM1.3 uveal melanoma cells colony formation in soft agar after shRNA-mediated knockdown of YAP. shRNA positive cells (control and YAP#1 and YAP#2) expressed Tomato (red) (left panel),

and were counted (right upper panel) (mean ± SEM, n = 10) and size measured (right lower panel) with Image-J (mean ± SEM, n = 20–100 colonies). (E) OMM1.3 uveal melanoma formation *in vivo* in cells expressing control and YAP shRNAs. Tumor size at the end of the study was measured (mean ± SEM, n = 6) (upper panel); H&E-stained sections of representative tumors from each group are shown (lower panel). (F) Soft agar assays show the effect of VP treatment on OMM1.3 uveal melanoma cells colony formation ability (left panel) and colony size (mean ± SEM, n = 20–50 colonies) (right panel). (G) Effect of VP on OMM1.3 uveal melanoma cells growth *in vivo*. Tumor size was measured every four days after the initiation of the VP treatment and control (mean ± SEM, n = 6) (n = numbers of tumors analyzed) (left panel). H&E-stained sections of representative tumors from each group (right panels). (H) Effect of VP treatment on OMM1.3 uveal melanoma cells